Int. J. Heat Mass Transfer. Vol. 34, No. 10, pp. 2629–2639, 1991
Printed in Great Britain

0017–9310/91 $3.00+0.00

Thermal diffusion effects in turbulent partial condensation

P. KAIPING† and U. RENZ
Lehrstuhl für Wärmeübertragung und Klimatechnik, RWTH Aachen, Eilfschornsteinstr. 18, D-5100 Aachen, F.R.G.

(*Received* 5 *June* 1990)

Abstract—The coupled heat and mass transfer during partial filmwise condensation inside a vertical tube is examined. The experiments are performed with an iso-octane/nitrogen mixture at turbulent flow conditions. Special attention is paid to thermodynamic coupling due to thermal diffusion. It is found that even in turbulent flow thermal diffusion contributes significantly to the overall mass transfer rate when the temperature differences between the bulk flow and the cooled wall are large and the radial concentration gradients remain small. The experimental results are well reproduced by numerical solutions of the conservation equations with the appropriate coupling terms.

1. INTRODUCTION

INDUSTRIAL mass transfer operations are very often linked to heat transfer processes as for instance in drying, evaporation and partial condensation. Consequently all these processes will be influenced to some extent by coupling effects between heat and mass transfer. The interrelations can be (1) the enthalpy flux caused by mass transport, (2) changes in transport properties due to variations in temperature and composition and (3) heat and mass transport due to thermal diffusion (Soret effect) and diffusion thermo (Dufour effect).

Thermal diffusion and diffusion thermo have been known from kinetic theory since the beginning of this century: a temperature gradient in a gas mixture will not only cause a conduction heat flux but also a thermally induced mass flux of the different species of the mixture (thermal diffusion). Similarly a concentration gradient will produce a diffusional mass flux and an additional heat flux (diffusion thermo). A detailed deviation of the equations describing thermal diffusion and diffusion thermo can be found in the monograph by Grew and Ibbs [1].

Most papers on thermodynamic coupling effects are theoretical in nature dealing with special operations like chemical vapour deposition [2] or gas injection [3–6] and deposition of small amounts of impurities in high temperature equipment [7, 8]. The transport of submicrometre particles due to thermal forces (thermophoresis) which is related to thermal diffusion has widely been studied [9]. However, little attention has been paid to the influence of thermodynamic coupling on common mass transfer operations like drying and partial condensation.

The reasons for this might be the complexity of thermodynamic coupling effects and the assumption that in industrial equipment commonly operated at turbulent flow conditions molecular transport is insignificant. However, in the near wall region turbulence is damped out and high gradients of concentration and temperature prevail. Thus, thermal diffusion and diffusion thermo can acquire greater importance in the boundary layer close to the wall.

Using known heat and mass transfer relations Dallmeyer [10] derived expressions for thermal diffusion mass fluxes and diffusion thermo heat fluxes. These relations show that in air/steam mixtures the coupling can always be neglected because the thermal diffusion factor remains small. As the thermal diffusion factor depends mainly on the difference in the molecular mass of the two species under consideration, thermal diffusion effects are more pronounced in gas mixtures having large differences in the molecular mass of components. Consequently, in mixtures of nitrogen or air with organic solvents, coupling must be assumed to be significant even in turbulent flow. Theoretical calculations based on the conservation equations for turbulent flows of vapour/gas mixtures on flat surfaces by Renz [11, 12] and within pipes by Odenthal [13] confirm this statement.

In the following sections results of a fundamental investigation are presented looking mainly at the influence of thermal diffusion on mass transfer in partial condensation [14]. Measurements and numerical calculations of heat and mass transport were carried out for filmwise condensation of an iso-octane/nitrogen mixture in a condenser pipe. As the difference in molecular mass of the two components is relatively large (iso-octane, $M_V = 114$ kg kmol^{-1}; nitrogen, $M_G = 28$ kg kmol^{-1}) the thermal diffusion factor α_T is large also ($\alpha_T = 0.3$–0.5) and thermal diffusion can

† Present address: Bayer AG, ZF-T Prozeßtechnik, Leverkusen, F.R.G.

NOMENCLATURE

B	driving force [—]
c_p	specific heat capacity [J kg^{-1} K^{-1}]
d	tube diameter [m]
D	diffusion coefficient [m^2 s^{-1}]
g	gravitational acceleration [m s^{-2}]
h	heat transfer coefficient [W m^{-2} K^{-1}]
h	specific enthalpy [J kg^{-1}]
$\hat{h}$	total specific enthalpy [J kg^{-1}]
j''	diffusional flux [kg m^{-2} s^{-1}]
l	length of condenser tube [m]
L	characteristic length of film flow [m]
$\dot{m}$	mass flow rate [kg s^{-1}]
$\dot{m}''$	mass flux density [kg m^{-2} s^{-1}]
M	molecular mass [kg kmol^{-1}]
$\dot{n}''$	molar flux [kmol m^{-2} s^{-1}]
p	pressure [Pa]
$\dot{q}''$	heat flux density [W m^{-2}]
$\dot{Q}$	heat flux [W]
r	radial coordinate [m]
R	tube radius [m]
R_M	universal gas constant [J mol^{-1} K^{-1}]
T	temperature [K, °C]
u	axial velocity [m s^{-1}]
v	radial velocity [m s^{-1}]
y	distance from interface or tube wall [m]
z	axial coordinate [m].

Greek symbols

α_T	thermal diffusion factor [—]
β	mass transfer coefficient [m s^{-1}]
δ	film thickness [m]
ζ	friction coefficient [—]
η	dynamic viscosity [kg m^{-1} s^{-1}]
λ	thermal conductivity [W m^{-1} K^{-1}]
ξ	vapour mass fraction [—]
ρ	density [kg m^{-3}]
τ	shear stress [N m^{-2}]
Ψ	vapour mole fraction [—]
ω	dimensionless stream function [—].

Subscripts

D	diffusion
eff	effective (turbulent and molecular)
F	film
G	inert gas
I	interface
in	inlet
loss	loss
m	axial mean value
o	without mass transfer
out	outlet
R	refrigerant
t	turbulent
T	with respect to heat transfer
TD	thermal diffusion
V	vapour
w	wall
τ	with respect to momentum transfer
Ψ	with respect to mass transfer.

be expected to contribute to mass transfer. A comparison of theoretical and experimental results gives further insight into the influence of thermal diffusion on mass transport during partial condensation of organic solvents.

2. FORMULATION OF THE PROBLEM

2.1. *Differential equations*

Partial filmwise condensation of an iso-octane/nitrogen mixture is considered inside a vertical pipe with cocurrent downward flow of both the vapour/gas mixture and the condensate film. Condensation, heat transfer and friction will lead to concentration, temperature and velocity profiles in both phases as shown in Fig. 1. These profiles are described by two sets of conservation equations: one for the vapour/gas mixture and one for the condensate flow. Both flow domains are connected by coupling conditions at the interface. In the following the ideal gas law is assumed to be valid for the mixture and thermal radiation is neglected.

2.1.1. *Vapour/gas flow.* The differential equations for the vapour/gas flow are (terms related to mixture properties have no subscript):

continuity equation

$$\frac{\partial(\rho u)}{\partial z} + \frac{1}{r}\frac{\partial(\rho r v)}{\partial r} = 0; \tag{1}$$

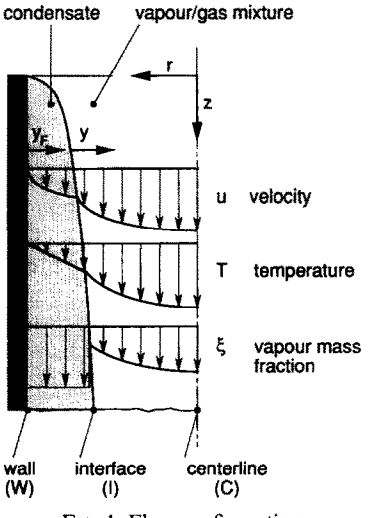

FIG. 1. Flow configuration.

z-momentum equation (velocity)

$$\rho u\frac{\partial u}{\partial z}+\rho v\frac{\partial u}{\partial r}=-\frac{1}{r}\frac{\partial(r\tau)}{\partial r}+\rho g-\frac{\mathrm{d}p}{\mathrm{d}z}; \quad (2)$$

energy equation (total enthalpy)

$$\rho u\frac{\partial \hat{h}}{\partial z}+\rho v\frac{\partial \hat{h}}{\partial r}=-\frac{1}{r}\frac{\partial(r\dot{q}''+ru\tau)}{\partial r}+\rho g z; \quad (3)$$

species conservation equation (vapour mass fraction)

$$\rho u\frac{\partial \xi}{\partial z}+\rho v\frac{\partial \xi}{\partial r}=-\frac{1}{r}\frac{\partial(rj'')}{\partial r}. \quad (4)$$

The formulation of the flux terms, τ, $\dot{q}''$ and j'' are given as follows:

shear stress

$$\tau=-\eta\frac{\partial u}{\partial r}-\eta_t\frac{\partial u}{\partial r}; \quad (5)$$

(↑ laminar friction; ↑ turbulent friction)

Heat flux

$$\dot{q}''=-\lambda\frac{\partial T}{\partial r}+(h_V-h_G)j''+\frac{M}{M_V M_G}\alpha_T R_M T j''-\frac{\eta_t}{Pr_t}c_p\frac{\partial T}{\partial r}; \quad (6)$$

(↑ conduction; ↑ diffusion; ↑ diffusion thermo; ↑ turbulent heat transport)

mass flux

$$j''=-\rho D\frac{\partial \xi}{\partial r}-\rho D\alpha_T\xi(1-\xi)\frac{1}{T}\frac{\partial T}{\partial r}-\frac{\eta_t}{Sc_t}\frac{\partial \xi}{\partial r}. \quad (7)$$

(↑ diffusion; ↑ thermal diffusion; ↑ turbulent diffusion)

The turbulent Prandtl and Schmidt numbers were taken to be 0.9.

The formulations for thermal diffusion and diffusion thermo were obtained from the kinetic theory of gases [15]. The thermal diffusion factor α_T is a property of the gas mixture depending on the two species, their concentrations and temperature. For a heavy vapour in a light gas α_T will be positive and the vapour will be forced towards the cooled wall. Potential models for the description of intermolecular forces are commonly used. These models are valid only for mono-atomic gases without internal degrees of freedom. Consequently, the accuracy of theoretical values of α_T is sometimes low for large molecules.

Because measurements in mixtures of organic solvents and air or nitrogen do not exist the α_T-values of the iso-octane/nitrogen mixture were calculated according to the first approximation of Chapman and Cowling, see ref. [15] with the Lennard–Jones-(6–12) potential.

2.1.2. *Liquid flow.* When the condenser tube is short enough, as was the case in the experiments, see ref. [14], the condensate flow remains laminar. For laminar vertical film flow the simplifications of the Nusselt theory can be used and the governing equations are:

continuity equation

$$\frac{\partial(\rho_F u_F)}{\partial z}+\frac{1}{r}\frac{\partial(r\rho_F v_F)}{\partial r}=0; \quad (8)$$

z-momentum equation

$$0=-\frac{1}{r}\frac{\partial\left(r\eta\frac{\partial u_F}{\partial r}\right)}{\partial r}+\rho_F g-\frac{\mathrm{d}p}{\mathrm{d}z}; \quad (9)$$

energy equation

$$0=\frac{1}{r}\frac{\partial\left(r\lambda\frac{\partial T_F}{\partial r}\right)}{\partial r}. \quad (10)$$

The species conservation equation reduces to

$$\xi_F=1 \quad (11)$$

because nitrogen is almost insoluble in liquid hydrocarbons.

2.1.3. *Boundary conditions.* The two sets of differential equations, equations (1)–(4) and (8)–(11), are subject to the following boundary and coupling conditions: at the wall the no-slip condition for u- and v-velocities has to be satisfied as well as a constant wall temperature (which was accomplished throughout the experiments). On the tube axis all gradients in the mixture flow will be zero because of symmetry arguments. At the interface the axial velocities, temperatures and pressures in the liquid and gaseous phase have to be equal. The corresponding vapour mass fraction results from the vapour pressure equation. Additionally, the shear stress and the heat and mass fluxes must be equal on both sides of the interface. The inlet conditions are taken from the experiment. They are a fully developed turbulent velocity profile and flat concentration and temperature distributions.

3. NUMERICAL METHOD

For the solution of the differential equations a computer program developed by Odenthal [13] was applied and matched to the problem. The numerical method of this program is based on a finite difference algorithm described by Patankar and Spalding [16]. The solution procedure is outlined here only in brief, details can be found in refs. [13, 14].

Instead of a solution of the conservation equations (1)–(4), a transformed set of equations is used where the radial coordinate r is replaced by the dimensionless stream function ω. The resulting set of partial differential equations has the general form

$$\frac{\partial\phi}{\partial z}+a_\phi(1-\omega)\frac{\partial\phi}{\partial\omega}=\frac{\partial}{\partial\omega}\left(c_\phi d_\phi\frac{\partial\phi}{\partial\omega}\right)+e_\phi+f_\phi\frac{\mathrm{d}p}{\mathrm{d}z} \quad (12)$$

where ϕ denotes the dependent variables u, $\hat{h}$ and ξ. Thermodynamic coupling terms are included in the source terms e_ξ and $e_{\hat{h}}$. The determination of coefficients d_ϕ requires the knowledge of the turbulent viscosity which is obtained from the k–ε turbulence model of Jones and Launder [17]. Thus, two additional equations of the form (12) have to be solved: one for the turbulent kinetic energy k and one for the turbulent energy dissipation ε. The model constants are taken from Kawamura [18].

The five equations (12) are discretized and put into a tridiagonal matrix form at every coordinate z_i

$$A_i\phi_{i+1}+\phi_i+B_i\phi_{i-1}=C_i+D_i\frac{\mathrm{d}p}{\mathrm{d}z} \tag{13}$$

for a numerical solution of the variables ϕ_i at positions ω_i. Making use of the inlet and boundary conditions and a previously determined value for the pressure gradient the system of equations is solved and the results are transformed back to the r–z coordinate system.

The solution of the film flow equations (8)–(10) goes in parallel to the equations of the gaseous phase because liquid and vapour gas flow are coupled at the interface. Taking the fluxes τ_1, $\dot{q}_1''$ and $\dot{m}_1''$ from the solution of the mixture flow it is possible to integrate the conservation equations of the film flow and the film thickness can be found iteratively. The new interface conditions u_1, T_1 and ξ_1 are then used as boundary conditions for the mixture flow at the next z-position.

This procedure has the advantage that the solution of the conservation equation need not be performed simultaneously in both flow domains. If the distance between two adjacent z-positions is small enough the chosen procedure does not introduce an error.

Apart from geometric dimensions the inlet velocity, the inlet temperature, the inlet mass fraction and the wall temperature are needed from experiments. In order to obtain a fully turbulent velocity profile at the inlet of the condenser section the adiabatic section in front of the condenser tube is calculated as well. At the entrance of this pipe section flat profiles are assumed and the turbulence intensity is taken to be 10%.

4. HEAT AND MASS TRANSFER AT THE INTERFACE

A solution of the differential equations will lead to temperature and mass concentration fields and hence to heat and mass transfer rates at the liquid interface. From these a heat transfer coefficient h and a mass transfer coefficient β can be derived

$$\dot{q}_1''=\left[-\lambda\frac{\partial T}{\partial r}+\frac{M}{M_V M_G}\alpha_T R_M T j''\right]_1 \tag{14}$$

$$\equiv h\,\Delta T \tag{15}$$

and

$$\dot{n}_{V,1}''=\frac{1}{M_V}\dot{m}_{V,1}''$$

$$=\frac{1}{M_V}\frac{\left[-\rho D\frac{\partial\xi}{\partial r}-\rho D\alpha_T\xi(1-\xi)\frac{1}{T}\frac{\partial T}{\partial r}\right]_1}{1-\xi_1} \tag{16}$$

$$\equiv\frac{\rho}{R_M T}\beta B_\Psi \tag{17}$$

where the driving force for mass transfer, B_Ψ, is defined as

$$B_\Psi=\frac{\Delta\Psi}{1-\Psi_1}. \tag{18}$$

For a comparison of experimental and theoretical results average values of the transport coefficients have to be determined. This requires the definition of mean temperature and mole fraction differences ΔT_m, $\Delta\Psi_m$. Both are taken to be the logarithmic mean differences evaluated with an average interface condition, e.g.

$$\Delta\Psi_m=\frac{\Psi_{in}-\Psi_{out}}{\ln\left(\frac{\Psi_{in}-\Psi_{l,m}}{\Psi_{out}-\Psi_{l,m}}\right)} \tag{19}$$

and

$$\Psi_{l,m}=\frac{1}{l}\int_0^l\Psi_l\,\mathrm{d}z. \tag{20}$$

The differences so defined were found to characterize the problem very well [14].

The experimental and theoretical results can now be presented in dimensionless form in terms of mean Sherwood and Nusselt numbers

$$Sh_m=\frac{\beta_m d}{D_m} \tag{21}$$

$$Nu_m=\frac{h_m d}{\lambda_m}. \tag{22}$$

All reference properties of the mixture are calculated using the average values of the mean inlet and outlet temperatures and concentrations, respectively.

The Nusselt and Sherwood numbers obtained numerically or experimentally can also be compared to heat and mass transfer laws like the formula derived by Gnielinski [19, 20]

$$Nu_{o,m}=\frac{\zeta/8(Re_m-1000)Pr_m}{1+12.7\sqrt{(\zeta/8)}(Pr_m^{2/3}-1)}\left[1+\left(\frac{d}{l}\right)^{2/3}\right] \tag{23}$$

with

$$\zeta=[1.82\log(Re_m)-1.64]^{-2} \tag{24}$$

or the corresponding mass transfer law for $Sh_{o,m}$ (assuming the analogy between heat and mass transfer to be valid). Here, the subscript o denotes ideal conditions, i.e. heat and mass transfer are not influenced by coupling effects.

If mass transfer is large Nu and Sh will be altered. The condensation mass flux towards the liquid interface changes the flow field leading to steeper gradients at the surface. Therefore, heat, mass and momentum transfer are increased. Common correction factors that take these effects into account can be obtained from film theory

$$\frac{Sh_m}{Sh_{o,m}} = \frac{\beta_m}{\beta_{o,m}} = \frac{1}{B_{\Psi,m}} \ln \frac{1}{1-B_{\Psi,m}} \tag{25}$$

$$\frac{Nu_m}{Nu_{o,m}} = \frac{h_m}{h_{o,m}} = \frac{1}{B_{T,m}} \ln \frac{1}{1-B_{T,m}} \tag{26}$$

where

$$B_{T,m} = \frac{\dot{m}''_{V,I,m} c_{pV}}{h_m}. \tag{27}$$

These simple corrections have been found to describe the changes due to diffusional mass flux quite well at moderate and high values of B_Ψ.

At low B_Ψ, however, thermal diffusion may have an effect on mass transfer. In partial condensation of a heavy vapour out of a mixture with a light non-condensable gas one would expect an increase in mass transfer because the heavier species will be forced towards the cooler region by thermal diffusion.

The relative importance of thermal diffusion can be estimated by analogy considerations from the transport terms if the ratio of the gradients of the dimensionless temperatures and molar fractions are replaced by Nusselt and Sherwood numbers. This yields [8, 10, 14]

$$\left[\frac{j''_{TD}}{j''_D}\right]_I = \alpha_{T,I,m}\left(\frac{T_m}{T_{I,m}} - 1\right)\Psi_{I,m} \frac{1}{B_{\Psi,m}} \left(\frac{Pr_m}{Sc_m}\right)^{1/3} \tag{28}$$

if Nu_m and Sh_m are assumed to be approximately proportional to $Pr_m^{1/3}$ and $Sc_m^{1/3}$, respectively.

Thermal diffusion, however, makes the analogy inapplicable and flattens the concentration gradient. This fact was found by Rosner [8] for the case of very low vapour concentrations and he introduced a correction for a 'pseudo sink' in his theoretical investigations. Röhl [21] was able to show the decrease of the concentration gradient in laminar flow. The flattened gradient was also found in the calculations of this paper for turbulent flow.

The decrease of the concentration gradient leads to a relative increase of thermal diffusion mass flux. However, it should be noted that overall mass transfer does not increase accordingly because ordinary (concentration) diffusion is lowered. This might be one reason for the fact that other authors have not realized thermal diffusion in their measurements.

In the experiments and calculations outlined in the next sections the changes in Sherwood number due to thermal diffusion will be investigated.

5. EXPERIMENTS

5.1. *Experimental set-up*

The experimental set-up is shown in Fig. 2. The main part of the apparatus is the condenser test section (1). The condenser was made of a copper tube 500 mm long and 40 mm i.d. and an outer steel jacket. The test section was insulated from the hot tubing of the apparatus by thick PTFE gaskets. Cooling was accomplished with an evaporating film of refrigerant R113 on the outside of the tube (see also Fig. 4). The evaporating refrigerant keeps the copper wall at a temperature of approximately 50°C. The condenser test section (1) is passed by the circulating turbulent mixture flow. This mixture is produced by combining the iso-octane vapour and nitrogen flows. The iso-octane is taken from the knock-out condenser (2) and pumped (3) into the evaporator (4). The superheated vapour passes a well insulated and heatable conduit (5) and enters the mixing tube (6). The nitrogen is circulated by a blower (7) and warmed up in a heat exchanger (8) before it is mixed with the vapour.

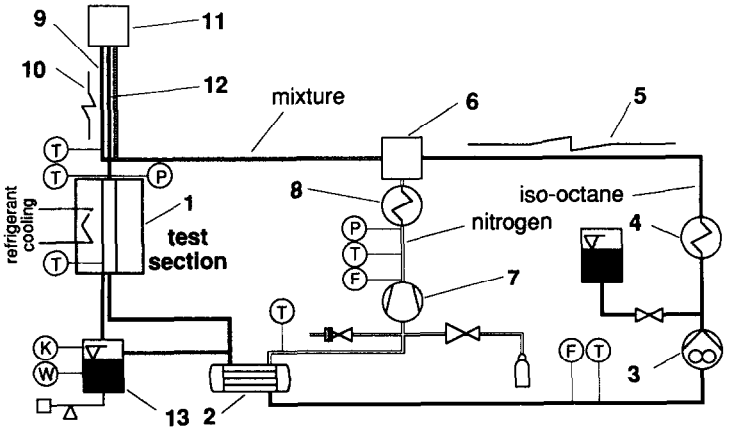

FIG. 2. Experimental set-up.

The hot vapour/gas mixture flows upwards in a tubular shell (9) on the outside of the inner pipe. The shell tube is well insulated and can be heated (10) in order to prevent the mixture from condensation. After a change in flow direction the mixture passes a calming chamber (11) and enters an isothermal section (12) of 40 mm diameter and approximately 70 diameters long now flowing vertically downward towards the condenser test tube (1). This type of design has the advantage that the hot upflow thermally insulates the fluid in the inner tube. Flat temperature profiles and a fully developed turbulent flow are obtained at the inlet of the test section.

In the test section, part of the vapour condenses. The condensate flow rate is measured on the scales (13) and then fed back to the liquid flow loop. The mixture exiting the test section is split up again into an iso-octane and nitrogen flow in the knock-out condenser (2). Measurements of temperatures, pressures, and flow rates were taken at various positions in the flow loop (see Fig. 2). All temperatures were measured with calibrated chromel/alumel thermocouples having an accuracy of approximately 0.1 K. Flowmeters were also calibrated before the experiment. Tube wall temperatures were measured with 0.5 mm thermocouples at nine positions within the tube wall. It was found that temperature variations between these positions were usually less than 0.5 K. The inaccuracy in measuring the tube wall temperature instead of the required temperature of the inner surface was estimated to be insignificant, i.e. less than 0.02 K.

A heat balance for the refrigerant yielded the heat flux across the tube wall. Heat loss across the outer insulation was determined in calibration experiments. From these calibration experiments the accuracy of the heat transfer measurements could be estimated to be better than 10 W. Experiments were performed with a mixture of iso-octane of 99.77% purity and technical grade nitrogen.

6. EVALUATION METHOD

6.1. *Heat and mass balances*

The determination of heat and mass transfer rates requires data about the inlet and outlet properties of the mixture, the liquid interface condition and the mass flow rates of mixture and condensate. Most of these values can be obtained directly by measurements, others are calculated from heat and mass balances. Where reference values are needed, they are calculated from the average of mean inlet and outlet values. The properties of the gas/vapour mixture and the condensate are evaluated as presented in ref. [14].

The heat flow through the tube wall is determined from a heat balance in the refrigerant cycle (Fig. 3)

$$\dot{Q}_w = \dot{m}_{R,V}(h_{R,V} - h_{R,in}) + \dot{m}_{R,out}(h_{R,out} - h_{R,in}) + \dot{Q}_{loss}. \quad (29)$$

From measured flow rates, pressures and temperatures, the inlet mass flow and the inlet properties are calculated. A species balance about the condenser tube gives the outlet flow rate of vapour

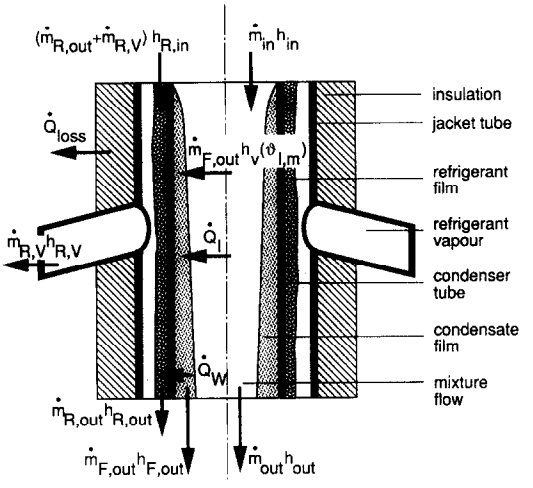

FIG. 3. Heat and mass balances.

$$\dot{m}_{V,out} = \dot{m}_{V,in} - \dot{m}_{F,out} \quad (30)$$

and consequently the mass fractions ξ_V and ξ_G at the exit of the condenser. The heat balance

$$\dot{m}_{out}h_{out} = \dot{m}_{in}h_{in} - \dot{m}_{F,out}h_{F,out} - \dot{Q}_w \quad (31)$$

can be used to determine the mean outlet enthalpy and temperature.

6.2. *Film flow*

For the evaluation of heat and mass transfer coefficients the interface condition of the liquid film has to be known. If the surface temperature of the film is approximately constant it can be calculated from the heat flow across the wall

$$T_{l,m} = \frac{\dot{Q}_w}{h_{F,m}\pi dl} + T_w. \quad (32)$$

The Nusselt theory will help to derive an equation for the unknown liquid film heat transfer coefficient $h_{F,m}$. This procedure is outlined in the following: starting from the momentum equation for the film flow, an equation for the outlet film thickness is obtained

$$\frac{\dot{m}_{F,out}}{\pi d} = \frac{g\rho_{F,m}^2}{3\eta_{F,m}}\delta_{out}^3 + \frac{\tau_{l,m}\rho_{F,m}}{\eta_{F,m}}\delta_{out} \quad (33)$$

which has to be solved iteratively. The shear stress can be calculated from the Blasius formula

$$\frac{\tau_{l,m,o}}{\rho_m u_m^2} = \frac{0.03955}{Re_m^{0.25}} \quad (34)$$

which should be corrected for mass transfer effects in analogy to equation (26).

Having δ_{out} it is possible to calculate the film Nusselt number at the exit of the condenser according to the formula

$$Nu_{F,out} = \frac{h_{F,out}L}{\lambda_{F,m}} = \frac{L}{\delta_{out}} \tag{35}$$

with the characteristic length

$$L = \left[\frac{(\eta_{F,m}/\rho_{F,m})^2}{g}\right]^{1/3}. \tag{36}$$

The relationship between average and outlet Nusselt number is found to be (see ref. [20])

$$Nu_{F,m} = 2\frac{2\frac{\delta_{out}}{L} + 3\frac{\tau_{I,m}}{g\rho_{F,m}}}{3\frac{\delta_{out}}{L} + 4\frac{\tau_{I,m}}{g\rho_{F,m}}} \tag{37}$$

which yields the required value for $h_{F,m}$

$$h_{F,m} = \frac{\lambda_{F,m}}{L} Nu_{F,m}. \tag{38}$$

It was shown in ref. [14] that the assumption of constant interface temperature can be accepted and that the experimental values $T_{I,m}$ according to equation (32) are almost indistinguishable from values calculated numerically.

6.3. *Dimensionless groups*

The Sherwood and Nusselt numbers are calculated from equations (21) and (22) with

$$\beta_m = \frac{\dot{m}_{F,out}}{M_V \pi d l \frac{p_m}{R_M T_m} B_{\Psi,m}} \tag{39}$$

and

$$h_m = \frac{\dot{Q}_I}{\pi d l \Delta T_m}.$$

The sensible heat $\dot{Q}_I$ is obtained from a heat balance about the condensate film (Fig. 4)

$$\dot{Q}_w = \dot{Q}_I + \dot{m}_{F,out}[h_V(T_{I,m}) - h_{F,out}]. \tag{40}$$

For a comparison of the experiments with heat and mass transfer laws equation (23) is used and correction factors are calculated according to equations (25) and (26). Additionally, the results are compared to numerical values obtained from the computer program.

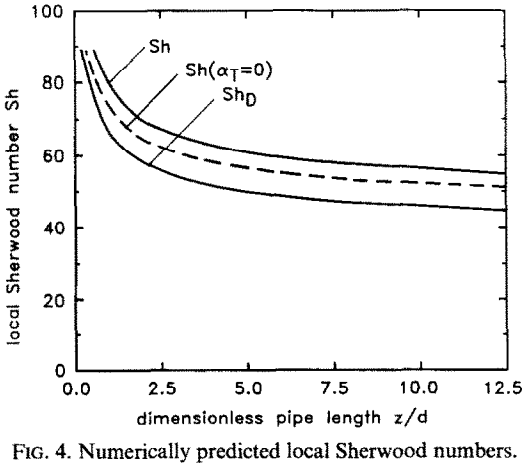

FIG. 4. Numerically predicted local Sherwood numbers.

7. RESULTS

7.1. *Numerical experiments*

The numerical calculations permit a more detailed look at the influence of different parameters which cannot be achieved by experiments: by setting the thermal diffusion factor to zero ($\alpha_T = 0$) one is able to simulate situations without thermal diffusion and compare these to real situations ($\alpha_T \neq 0$) as would be found in experiments.

The result of one such calculation is presented in Fig. 4 where local Sherwood numbers are plotted vs the dimensionless length of the condenser tube. Due to thermal diffusion the mass transfer is increased and the local Sherwood number is larger than the one calculated with $\alpha_T = 0$.

However, it is interesting to note that the diffusional part of the mass transfer represented by Sh_D is lowered when thermal diffusion is included. Although in this example thermal diffusion contributes to some extent to mass transfer, the total amount of condensate is increased only very little compared to a calculation with negligible thermal diffusion. Thus, thermal diffusion acts in two ways: it adds to total mass transfer but it also reduces the diffusional flux by decreasing the concentration gradients.

The change in concentration profiles can be explained if one looks at the species conservation equation (4): the inclusion of the additional transport in the radial flux term changes the balance between convective fluxes on the left-hand side and the radial transport on the right-hand side of the equation. Consequently convection and radial transport have to be adjusted to a new balance by a change of the concentration profile. Rosner [8] used a similar argument when he reformulated the species conservation equation. Assuming that the vapour is present in traces only, he split up the thermal diffusion flux term in a 'pseudo sink' which he attributed to convection and a 'pseudo source' which he added to radial diffusion.

Figure 4 gives the general idea on how mass transfer in partial condensation is altered by thermal diffusion. Now the influence of various parameters on condensation rates will be discussed.

From equation (28) the following correlation for the changes in mass transfer can be obtained:

$$\frac{Sh_m}{Sh_m(\alpha_T = 0)} \approx 1 + \alpha_{T,I,m}\left(\frac{T_m}{T_{I,m}} - 1\right)\Psi_{I,m}\frac{1}{B_{\Psi,m}}\left(\frac{Pr_m}{Sc_m}\right)^{1/3} \tag{41}$$

where $Sh_m(\alpha_T = 0)$ is a reference Sherwood number

for diffusional mass transfer which would be predicted if coupling is neglected, and the value 1 is used as an approximation for $Sh_{D,m}/Sh_m(\alpha_T = 0)$.

Equation (41) shows the parameters that determine the effect of thermal diffusion and should be varied in this investigation. Because a variation in interface properties changes all other parameters as well, the interface temperature was kept approximately constant by choosing a fixed wall temperature, $T_w = 50°C$, throughout the calculations and experiments. With the selected vapour/gas system $\alpha_{T,l,m}$ was thereby also fixed.

In Fig. 5 graphs are presented for $Sh_m/Sh_m(\alpha_T = 0)$ as a function of the temperature parameter $(T_{in}/T_w - 1)$ which was used as an approximation of $(T_m/T_{l,m} - 1)$.

Although the linear dependency predicted by equation (41) (using $\alpha_{T,l,m} = 0.33$, $Pr/Sc = 1.15$ and $\Psi_{l,m} = 0.22$) cannot be confirmed exactly, a clear increase in Sherwood number with increasing temperature parameter can be detected.

The ratio $Sh_m/Sh_m(\alpha_T = 0)$ shows only the net increase in mass transfer due to thermal diffusion. In order to detect the real contribution of thermal diffusion to mass transfer one has to look at the ratio between overall and diffusional Sherwood number, $Sh_m/Sh_{D,m}$. Agreement between this ratio (dashed curve in Fig. 5) and equation (41) is better, indicating the high contribution of thermal diffusion to mass transfer. However, curves of this type are inconvenient in practice as they need a reference value $Sh_{D,m}$ that can only be calculated numerically. Additionally, they do not indicate the net effect of thermal diffusion which is the value of main interest.

The influence of the mass transfer driving force $B_{\Psi,m}$ is shown in Fig. 6. Here two sets of graphs are presented in order to show a dependency on Reynolds number of the mixture flow which is not explicitly given as a parameter in equation (41). For increasing $1/B_{\Psi,m}$ we find the expected increase in mass transfer. The influence of Reynolds number is almost negligible. Again, the discrepancy to the predictions by

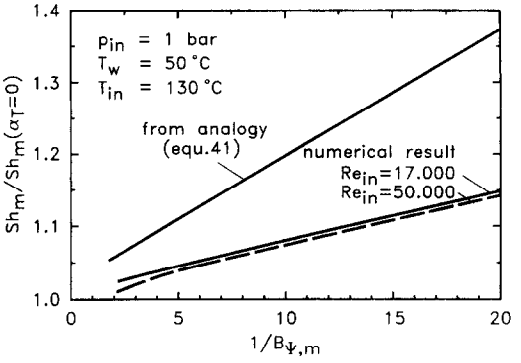

FIG. 6. Influence of mass transfer driving force on thermal diffusion effect.

equation (41) is due to the fact that this formula does not take into account the decrease in diffusional flux.

7.2. *Comparison of experimental and theoretical mass transfer*

In order to present the measured mass transfer rates a convenient choice of the reference Sherwood number has to be made. As there are no experiments without thermal diffusion an empirical Sherwood number at vanishing mass transfer rates according to equation (23) was chosen. This equation was shown to represent our theoretical mass transfer results for systems in which thermodynamic coupling can be neglected with an error of less than 10% for all mass transfer driving forces and all inlet temperatures when used in connection with film theory. For a mass transfer driving force $B_{\Psi,m} < 0.1$, the region of largest interest for this study, the error is even smaller than 5% [13].

In Fig. 7 experimental and theoretical mass transfer results are presented in the form of $Sh_m/Sh_{o,m}$ for the system iso-octane/nitrogen over $B_{\Psi,m}$. The tube inlet temperature was taken as an additional parameter. Wall temperature as well as overall pressure and Reynolds number were kept constant in these experiments.

At high values of the driving force $B_{\Psi,m}$ the influence of the diffusional fluxes is well described by film

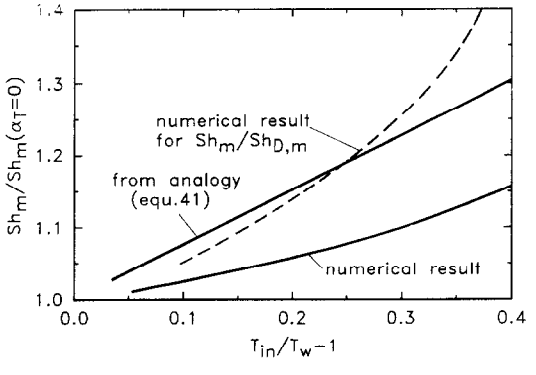

FIG. 5. Influence of temperature ratio on thermal diffusion effects.

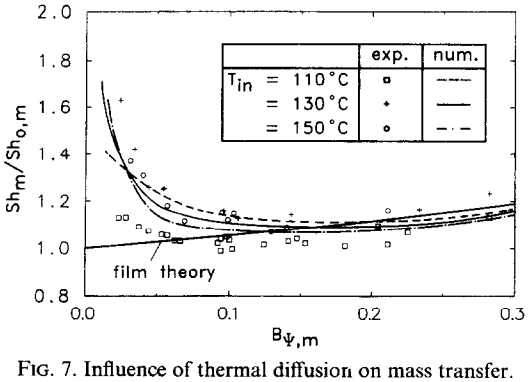

FIG. 7. Influence of thermal diffusion on mass transfer.

theory. At low $B_{\Psi,m}$, however, theoretical and experimental values depart strongly from the empirical mass transfer law due to thermal diffusion effects. Consequently values of $Sh_m/Sh_{m,o}$ very much larger than unity are obtained in the experiments as well as in the numerical calculations.

Although theoretical and experimental data do not match completely their behaviour is quite similar. The influence of the higher temperature gradient at inlet temperatures of 150 and 130°C is very pronounced in the experiments. The calculations show the same form only for values of $B_{\Psi,m} < 0.03$. This might be due to slightly inaccurate predictions of the thermal diffusion factor α_T. In general, however, theory and experiment give clear evidence of the thermal diffusion effects at low $B_{\Psi,m}$.

That these effects are not changed by Reynolds number can be seen from Fig. 8 which was obtained for a mass transfer driving force of $B_{\Psi,m} = 0.1$ and an inlet temperature of $T_{in} = 130$°C. In this diagram the experimental results for different Reynolds numbers in the turbulent flow regime are presented together with theoretical data of (a) calculations taking thermal diffusion into account, (b) calculations neglecting thermal diffusion and (c) the Gnielinski mass transfer law with correction for wall mass flux (film theory). For all Reynolds numbers the experiments are well predicted by theory when thermal diffusion is included in the calculations. If thermal diffusion is neglected the calculated mass transfer remains too small—in these experiments the deviations are approximately 10–15%.

The Gnielinski formula seems to have a slightly different slope, leading to smaller values at lower and higher values at larger Reynolds numbers. This behaviour was found throughout the investigation (see also ref. [14]). Finally, it should be mentioned that the results of all mass transfer experiments were numerically predicted with a maximum error of 10% if thermal diffusion was included in the calculations.

7.3. *Comparison of experimental and theoretical heat transfer*

This investigation would not be complete without a brief report on heat transfer results. The sensible heat flow across the liquid film interface was small—commonly in the range of 100–300 W. Consequently, heat transfer data cannot be as accurate as mass transfer data.

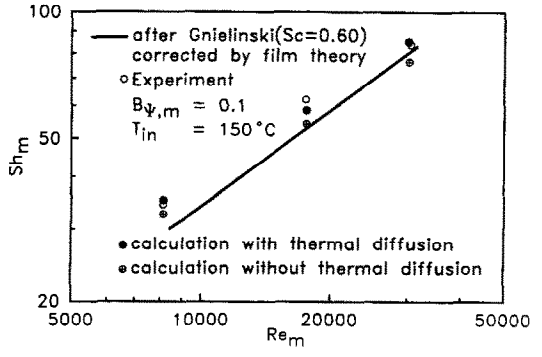

FIG. 8. Influence of Reynolds number on thermal diffusion effects.

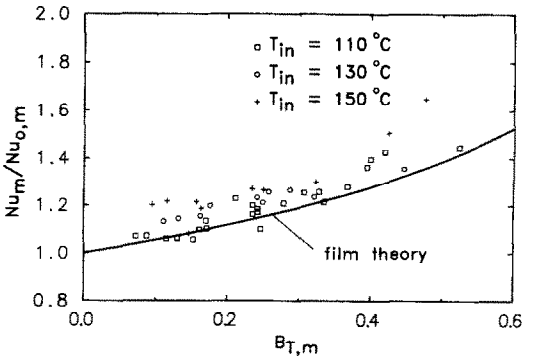

FIG. 9. Sensible heat transfer in partial condensation of isooctane/nitrogen mixtures.

In Fig. 9 the experimental heat transfer results are presented in the form of Nusselt number ratios as a function of the heat transfer driving force $B_{T,m}$ and compared to film theory. The reference Nusselt number $Nu_{o,m}$ was evaluated according to equation (23). In general, the agreement of the experiments with film theory is good although the experiments give slightly higher Nusselt numbers. The experimental heat transfer data were also found to be mostly larger than the numerical predictions which were omitted for clarity. Deviations were, however, rarely larger than 10%. Thus, an error in the experimental data of about 10% might have occurred due to experimental difficulties in measuring the small heat flow rates.

8. CONCLUSION

Measurements and experiments show that thermal diffusion can play an important role in mass transfer during partial condensation even in the turbulent flow of gas/vapour mixtures with large differences in molecular masses. In such cases condensate flow rates can be significantly increased by thermal diffusion when the driving force for mass transfer B_Ψ remains small and temperature gradients are large. Common estimation formulae are not too far off when predicting the real influence of thermal diffusion. As they do not take into account the reduction in diffusional flux caused by thermal diffusion, the net effect of thermal diffusion is usually smaller than expected. It is this behaviour that has led to the common, although sometimes inaccurate neglect of thermal diffusion in mass transfer processes.

Acknowledgement—The financial support of the 'Deutsche Forschungsgemeinschaft' (German Science Foundation), is gratefully acknowledged.

REFERENCES

1. K. E. Grew and T. L. Ibbs, *Thermal Diffusion in Gases*. Cambridge University Press, London (1952).

2. J. P. Jenkinson and R. Pollard, Thermal diffusion effects in chemical vapor desposition reactors, *J. Electrochem. Soc.* **131**, 2911–2917 (1984).
3. E. R. G. Eckert, Thermodynamische Kopplung von Stoff- und Wärmeübergang, *Forsch. IngWes.* **29**, 147–151 (1963).
4. E. M. Sparrow, W. J. Minkowycz, E. R. G. Eckert and W. E. Ibele, The effect of diffusion thermo and thermal diffusion for helium injection into plane and axisymmetric stagnation flow of air, *J. Heat Transfer* **86**, 311–319 (1964).
5. E. M. Sparrow, W. J. Minkowycz and E. R. G. Eckert, Transpiration-induced buoyancy and thermal diffusion–diffusion thermo in a helium–air free convection boundary layer, *J. Heat Transfer* **86**, 508–514 (1964).
6. A. Atimtay and W. N. Gill, The effect of free stream concentration on heat and binary mass transfer with thermodynamic coupling in forced convection on a flat plate, *Chem. Engng Sci.* **36**, 1001–1008 (1981).
7. R. Srivastava and D. E. Rosner, A new approach to the correlation of boundary layer mass transfer rates with thermal diffusion and/or variable properties, *Int. J. Heat Mass Transfer* **22**, 1281–1294 (1979).
8. D. E. Rosner, Thermal (Soret) diffusion effects on interfacial mass transport rates, *PhysicoChem. Hydrodyn.* **1**, 159–185 (1980).
9. L. Talbot, Thermophoresis—a review, *Prog. Astronaut. Aeronaut.* **74**, 467–488 (1981).
10. H. Dallmeyer, Stoff- und Wärmeübertragung bei der Kondensation eines Dampfes aus einem Gemisch mit einem nicht kondensierenden Gas in laminarer und turbulenter Strömungsgrenzschicht, *VDI ForschHft* **539** (1970).
11. U. Renz, Verdunstung mit und ohne Zerfallstreaktion der Flüssigkeit, Dissertation, Universität Stuttgart (1970).
12. U. Renz, Die partielle Filmkondensation aus laminaren und turbulenten Grenzschichtströmungen, *Lett. Heat Mass Transfer* **2**(1), 9–12 (1975).
13. H.-P. Odenthal, Berechnung des Wärme- und Stoffaustauschs bei partieller Kondensation im turbulent durchströmten Kondensatorrohr, Dissertation, RWTH Aachen (1983).
14. P. Kaiping, Der Einfluß der Thermodiffusion auf die Teilkondensation in einer turbulenten Rohrströmung, Dissertation, RWTH Aachen (1988).
15. E. A. Mason, Transport in neutral gases. In *Kinetic Processes in Gases and Plasmas* (Edited by A. B. Hochstim). Academic Press, New York (1969).
16. S. V. Patankar and D. B. Spalding, *Heat and Mass Transfer in Boundary Layers*, 2nd Edn. Intertext, London (1970).
17. W. P. Jones and B. E. Launder, The prediction of laminarization with a two-equation model of turbulence, *Int. J. Heat Mass Transfer* **15**, 301 314 (1972).
18. H. Kawamura, Analysis on laminarization of heated gas using a two-equation model of turbulence, 2nd Symp. on Turbulent Shear Flow, Imperial College London, pp. 1816–1821 (1979).
19. V. Gnielinski, Neue Gleichungen für den Wärme- und Stoffübergang in turbulent durchströmten Rohren und Kanälen, *Forsch. IngWes.* **41**, 8–16 (1975).
20. *VDI-Wärmeatlas, Berechnungsblätter für den Wärmeübergang*, 4. Aufl. VDI, Düsseldorf (1984).
21. L.-P. Röhl, Einfluß von Thermodiffusion, Diffusionsthermik und Enthalpietransport auf den Stoff- und Energietransport in binären Gemischen bei laminarer Rohrströmung, Dissertation, TU Berlin (1971).

EFFETS DE LA DIFFUSION THERMIQUE DANS LA CONDENSATION PARTIELLE TURBULENTE

Résumé—On examine le transfert couplé de chaleur et de masse pendant la condensation partielle en film dans un tube vertical. Les expériences sont conduites avec un mélange iso-octane/azote dans des conditions d'écoulement turbulent. Une attention particulière est portée au couplage thermodynamique dû à la diffusion thermique. On trouve que même en écoulement turbulent, la diffusion thermique contribue significativement au flux de masse globalement transféré quand les différences de température entre ie coeur de l'écoulement et la paroi froide sont grandes et les gradients radiaux de concentration demeurent petits. Les résultats expérimentaux sont bien reproduits par des solutions numériques des équations de bilan avec les termes de couplage appropriés.

EINFLUSS DER THERMODIFFUSION BEI DER TURBULENTEN PARTIELLEN KONDENSATION

Zusammenfassung—Die Kopplung des Wärme- und Stoffaustauschs bei der partiellen Filmkondensation eines Iso-Oktan/Stickstoff-Gemischs wird für ein senkrechtes, turbulent durchströmtes Rohr untersucht. Dabei interessiert vor allem der Einfluß der Thermodiffusion auf den Stoffaustausch. Es konnte experimentell nachgewiesen werden, daß auch in turbulenten Strömungen die Thermodiffusion die Größenordnung der konzentrationsbedingten Diffusion erreichen kann, wenn bei großen Temperaturdifferenzen die Konzentrationsdifferenzen zwischen Kernströmung und gekühlter Wand klein bleiben. Der experimentelle Befund wird durch theoretische Voraussagen auf der Grundlage einer numerischen Lösung der um die Kopplungsterme erweiterten Erhaltungsgleichungen für die turbulente Rohrströmung bestätigt.

ЭФФЕКТЫ ТЕРМОДИФФУЗИИ ПРИ КОНДЕНСАЦИИ В ТУРБУЛЕНТНОМ РЕЖИМЕ

Аннотация—Исследуется взаимосвязанный тепло- и массоперенос при пленочной конденсации из смеси в вертикальной трубе. Эксперименты проводились со смесью изооктан-азот в условиях турбулентного течения. Особое внимание уделялось термодинамическому взаимодействивию, обусловленному термодиффузией. Найдено, что даже при турбулентном течении вклад термодиффузии в скорость суммарного теплопереноса является значительным, если разность температур объемного потока и охлаждаемой стенки велика, а поперечные градиенты концентрации остаются малыми. Экспериментальные результаты хорошо согласуются с численными решениями уравнений сохранения с соответствующими взаимосвязанными слагаемыми.